J Mater Sci (2011) 46:2635–2643
DOI 10.1007/s10853-010-5118-8

A sustained folic acid release system based on ternary magnesium/zinc/aluminum layered double hydroxides

Rong Xiao · Wenrui Wang · Longlong Pan · Rongrong Zhu · Yongchun Yu · Huiping Li · Hui Liu · Shi-Long Wang

Received: 29 August 2010 / Accepted: 26 November 2010 / Published online: 22 December 2010

Abstract This study first synthesized and characterized the ternary magnesium/zinc/aluminum layered double hydroxides (Mg/Zn/Al-LDHs) intercalated with folic acid. We prepared the ternary (Mg, Zn, Al) LDH carrier by the introduction of zinc, because magnesium and zinc are both vital minerals of human body. The nanohybrids were prepared by the method of coprecipitation and were characterized by powdered sample X-ray diffraction (XRD), Fourier transform infrared spectra (FT-IR), UV–vis spectra, and MTT assay. The loading amount of intercalated folic acid was increased to 45.2%, and showed a profile of sustained release with 75% in 250 min. In addition, the folic acid-LDH nanohybrids showed an enhanced thermal stability and a profound buffering property, which demonstrated that the hybrids could protect folic acid against heat degradation and prompt its available diffusion. The cell viability of HEK293T was over 80% after treated with nanohybrids for 72 h. Our results suggested that the ternary folic acid-LDH nanohybrids may function as a useful nutritional tablet to promote the bioavailability of folic acid delivery.

Rong Xiao and Wenrui Wang contributed equally to this study.

R. Xiao · W. Wang · L. Pan · R. Zhu · Y. Yu · H. Li · S.-L. Wang (✉)
Tenth People's Hospital, School of Life Science and Technology, Shanghai Pulmonary Hospital, Tongji University, 1239 Siping Road, Shanghai 200092, People's Republic of China
e-mail: wsl@tongji.edu.cn

H. Liu (✉)
Eastern Hepatobiliary Surgery Hospital, Second Military Medical University, Shanghai 200438, People's Republic of China
e-mail: liuhuigg@hotmail.com

Introduction

Folic acid (Fig. 1), the supplemental form of a B complex vitamin, plays a crucial role in the prevention of disease. Previous reports [1–4] demonstrated that folic acid can prevent birth defects known as neural tube defects and other malformations. Folic acid supplementation can reduce plasma homocysteine levels and improve the total plasma antioxidant capacity in coronary artery disease and hemodialysis patients [5, 6], delay atherosclerotic lesion development [7], and lower blood pressure slightly [8, 9]. Many studies [10–12] have shown the inverse association between folic acid and cancer risk. The deficiency of folic acid causes DNA damage and higher incidence of carcinomas [13]. Also, folic acid deficiency may result in psychiatric symptoms and increase the severity of other mental diseases [14, 15]. Folic acid deficiency is mainly caused by its low daily intake from food, because 50 to 95% of folate is lost during prolonged storage and cooking. Therefore, many strategies have been employed to increase folic acid absorption with a carrier-mediated transport antacid [16, 17].

Layered double hydroxides (LDHs), commonly known as hydrotalcite-like materials or anionic clays, are a family of layered nanomaterials with wide application in catalysts, absorption, pharmaceutics, and photochemistry [18–20]. Recently, LDHs have received considerable attention as drug delivery system owing to its low cytotoxicity, good biocompatibility, and total protection of the loaded drugs [19, 21]. Many drugs have been successfully intercalated such as captopril, ascorbic acid, gliclazide, anti-inflammatory drugs fenbufen, anticoagulant heparin, and anticancer drugs podophyllotoxins [22–27]. Furthermore, the effectiveness of LDH as an antacid has already been reported [19]. Most LDH materials can be represented by

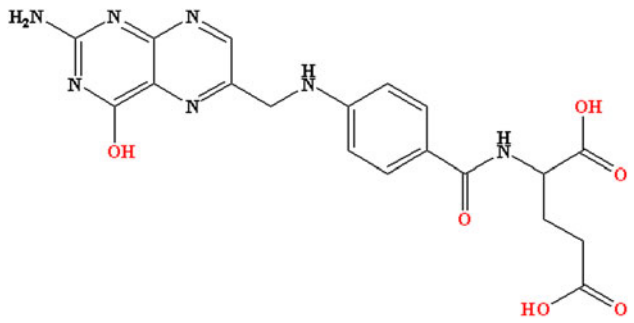

Fig. 1 Molecular formula of folic acid

the general formula $[M^{II}_{1-x}\ M^{III}_{x}\ (OH)_2]^{x+}\ (A^{m-})_{x/m}{\cdot}nH_2O$, where M^{II} is a divalent metal cation as Mg^{2+}, Zn^{2+}, Ni^{2+}, etc., M^{III} a trivalent metal cation as Al^{3+}, Fe^{3+}, Cr^{3+}, etc., and A^{m-} is interlayer anion as NO_3^-, CO_3^{2-}, and Cl^- [28, 29]. These materials can present different properties, depending on the kind of di and trivalent cations, their ratio and the ionic strength conditions, as well as the interlamellar anion [30, 31]. In this study, the ternary system Mg/Zn/Al-LDH was used instead of the reported Mg/Al-LDH, because Mg^{2+} and Zn^{2+} are vital minerals in many biological functions. Zinc is essential for the synthesis of DNA and protein, cell division, and metabolic activities of 300 enzymes [32, 33]. It is also critical to the tissue growth, the immune system function, and the fetal growth. Zinc deficiency may result in birth defects, growth retardation, cancer and depression [33, 34]. Magnesium, also an important element for health, can activate over 300 different biochemical reactions and protect against heart diseases, heart attacks, high blood pressure, stroke, and type II diabetes [35, 36].

In this study, the Mg/Zn/Al-LDHs intercalated with folic acid were synthesized. And after a set of characterizations, the buffer-effect and release behavior have been evaluated. The in vitro cell cytotoxicity was examined as well.

Materials and methods

Synthesis of Mg/Zn/Al-LDH

The samples were prepared after a coprecipitation method [37]. A mixed solution (10 mL) containing 0.15 M $Mg(NO_3)_2$, 0.15 M $Zn(NO_3)_2$, and 0.1 M $Al(NO_3)_3$ (M^{2+}/M^{3+} ratio, 3:1) was added into a solution (40 mL) of 0.17 M NaOH with vigorous stirring under nitrogen atmosphere at room temperature for 10 min. The resultant precipitates were centrifugated and washed twice with deionized water, then dispersed in 40 mL of double distilled water and treated in a autoclave at 50 °C for 12 h. The LDH solid was harvested by filtering and vacuum drying overnight.

Synthesis of folic acid–Mg/Zn/Al-LDH

The preparation of folic acid–Mg/Zn/Al-LDH followed a similar method. A mixed solution (40 mL) of 0.17 M NaOH and 0.1 M folic acid was stirring at room temperature for 10 min, and then a solution (10 mL) containing 0.15 M $Mg(NO_3)_2$, 0.15 M $Zn(NO_3)_2$, and 0.1 M $Al(NO_3)_3$ was added. The mixture was kept vigorous magnetically stirring under N_2 for 3 h. The resultant slurry was then treated, as aforementioned, including wash, and hydrothermal treatment. The product was denoted as folic acid-LDH.

Characterization

Powder X-ray diffraction (XRD) was recorded on a Rigaku Diffractometer Model Miniflex using CuKα source ($\lambda = 0.154060$ nm) at 40 mA and 40 kV. Fourier transform infrared spectra (FT-IR) were obtained on a Bruker Vector22 spectrophotometer using KBr pellet method (sample/KBr = 1/100) in the range of 4000–500 cm^{-1}. Thermogravimetry (TG) and differential thermal analysis (DTA) curves were recorded in flowing air with a heating rate of 10 °C/min on a Perkin-Elmer Pyris1 TG/DTA instrument. UV–vis spectra were measured on a CARY50 spectrophotometer.

Evaluation of the buffer effect

The pH, which changes in each suspension after the addition of 1 M HCl aqueous solution, was recorded to measure the buffer effect of folic acid-LDH [38, 39]. HCl aqueous solution was subsequently added to the suspension (10 mL) containing folic acid-LDH (100 mg) with continuously stirring at 37 °C, until pH stabilized at an approximate value of 1.

Determination of loading amount and in vitro release test

The amount of intercalated folic acid was determined by UV–vis spectroscopy. A known weight of nanohybrids was placed in a 10-mL flask, then 0.5 mL of 5 M HCl solution was added and the flask was filled with 0.02 M phosphate buffer solution. After the hybrids were totally dissolved, the concentration of folic acid was determined by monitoring the absorbance at 280 nm with a UV–vis spectroscopy. The concentration was calculated according to an already obtained standard curve of folic acid ($A = 0.09085\ C + 0.01227$, $r = 0.99962$).

The folic acid release test was performed in 200 mL of pH 7.4 phosphate buffer solution (0.02 M) containing 0.02 g folic acid-LDH at constant temperature 37 ± 1 °C. The paddle rotation speed was 100 rpm. Aliquots (2 mL)

were withdrawn at desired time intervals and filtered through a 0.45 μm syringe filter. The accumulated amount of folic acid released was determined by UV absorption at 280 nm. Four dissolution–diffusion kinetic models were used to fit the in vitro folic acid-LDH release profiles (Table 2). The zero- and first-order model are normally used to describe the dissolution phenomena, while the parabolic diffusion model expresses the diffusion-controlled release process and the modified Freundlich model elucidates the diffusion behavior via ion-exchange[40].

Cytotoxicity assay

Human Embryonic kidney (HEK 293T) cells were routinely cultured at 37 °C in the atmosphere of 5% CO_2 in the flasks containing 10 mL of DMEM growth medium supplemented with 10% Fetal bovine serum (FBS), 100U/mL penicillin, and 100 μg/mL streptomycin. At 80–90% confluence, cells were differentiated with trypsin–EDTA and plated at an optimum density of 1×10^4 cells per well in a 100 μL total volume of appropriate medium on 96 well. After incubation at 37 °C in a 5% CO_2 humid for 24 h, triplicate wells were treated with folic acid-LDH, free folic acid, and LDH in the various concentrations from 10 to 100 μg/mL. The plates were then incubated as described above for 24, 48, and 72 h, respectively. A control experiment was performed without treated under the same conditions. The number of living cells was determined by MTT assay with 3-(4,5-dimethylthiazole-2-yl)-2,5-phenyltetrazolium bromide. After cells incubated with 20 μL of MTT for 4 h under light-blocking condition, the medium was removed and 150 μL of DMSO was added into each well [41]. Absorbance was measured at 490 nm using ELX 800 reader, and cell viability was calculated by the following formula:

$$\text{Cell viability } (\%) = (\text{OD}_{490}(\text{test}) \,/\, \text{OD}_{490}(\text{control})) \times 100\%$$

The lactate dehydrogenase activity was used as an indicator of cell membrane integrity and serves as a general means to assess cytotoxicity resulting from nanohybrid effect after 72 h [42]. It was measured by the LDH Cytotoxicity Assay Kit.

This study to work on HEK293T cell line was approved by the Institutional Human Research Ethics Committee (HREC 02247/02267).

Results and discussion

XRD analysis

The powder XRD patterns for Mg/Zn/Al-LDH and its intercalated nanohybrid are presented in Fig. 2, and the basal spacing calculated from the XRD patterns are shown in Table 1. As shown in Fig. 2a, pristine Mg/Zn/Al-LDH exhibits the typical diffraction peaks of LDH compound [43]. The basal spacing d_{003} of 0.88 nm and d_{006} of 0.45 nm are similar to the values reported previously [44], which suggest that Mg/Zn/Al-LDH was well crystallized and high ordered. For pattern of folic acid-LDH in Fig. 2b, the reflection peaks shift to lower angles and become weaker. Also, it is observed that the successful intercalation of folic acid anions increases the basal spacing from 0.88 to 1.42 nm. Since the brucite-like layer thickness of LDH is 0.48 nm [45] and the gallery of height is calculated as 0.94 nm, which is shorter than the molecular length of folic acid (≈1.9 nm). So the folic acid molecules are arranged in tilted monolayer with tilting angles of about 60°, as illustrated in Fig. 3.

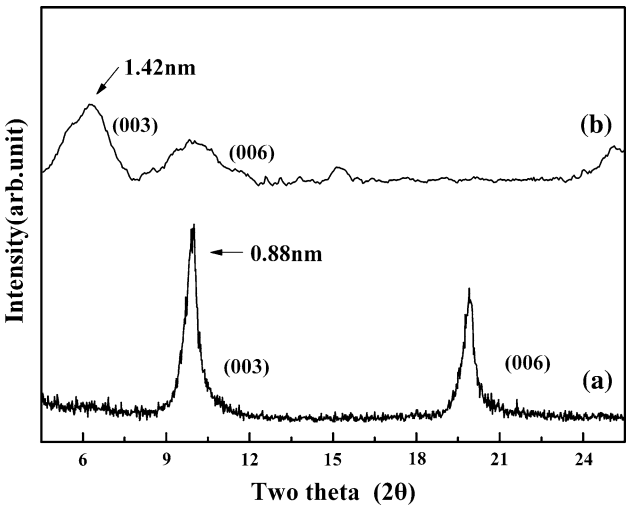

Fig. 2 Powder X-ray diffraction patterns for (*a*) Mg/Zn/Al-LDH and (*b*) Folic acid-LDH

As shown in Table 1, the loading amount of folic acid in ternary metal Mg/Zn/Al-LDH is 45.2%. Compare to our previous study [46], It is much higher than the amount intercalated into binary metal Mg/Al-LDH of 19.32%. It is possible that the attractive force between the positively charged brucite-like layer and the anion located in the interlayer region has become stronger, by introducing a cation of Zn^{2+} with higher electronegativity [43].

FT-IR and UV–vis spectroscopy

As shown in Fig. 4, all samples exhibit a broad absorption peak centered around 3400 cm^{-1}, which could be assigned to the presence of OH stretching modes of the hydroxide basal layer and water molecules. The Mg/Zn/Al-LDH (Fig. 4a) displays a sharp and intense absorption band at 1386 cm^{-1}, which is ascribed to the NO_3^- vibration. This absorption band disappeared in folic acid-LDH (Fig. 4b,

Table 1 The *d*-value of nanohybrid and folic acid loading

Nanohybrid	*d*-values/nm			Gallery height/nm	Folic acid loading/%,w/w
	d_{003}	d_{006}	d_{110}		
Mg/Zn/Al-LDH	0.884	0.446	0.153	0.404	–
Folic acid-LDH	1.42	0.791	0.152	0.940	45.2 ± 2.2%[a] (47.2[b])

[a] Measured by UV–vis spectroscopy; [b] calculated by TG–DTA profiles

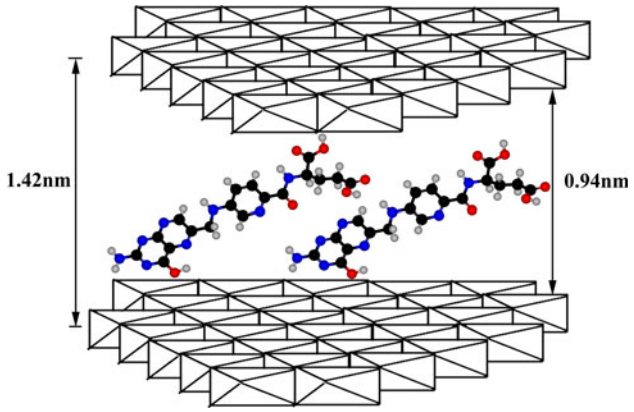

Fig. 3 Schematic structural model of folic acid-LDH

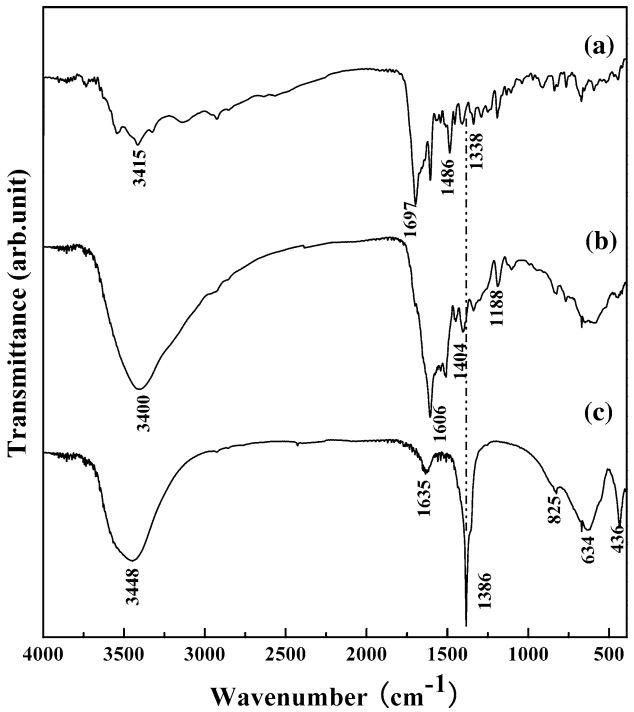

Fig. 4 The FT-IR spectra for (*a*) folic acid, (*b*) folic acid-LDH, and (*c*) Mg/Zn/Al-LDH

which indicates NO_3^- anion is completely replaced by folic acid anions. In the low-frequency region, the bands at 825, 634, and 436 cm^{-1} can be attributed to M–O and O–M–O vibration [28]. These bands can also be observed in folic acid-LDH (836, 645, and 439 cm^{-1}) with small shift, which results from the existence of host–guest interaction between the interlayer folic acid and hydroxyl groups of LDH layers [25]. In addition, the band at 1635 cm^{-1} is due to the H–O–H bending vibration [47]. The characteristic peaks around 1697 cm^{-1} presented in both folic acid and folic acid-LDH correspond to the (C=O) stretching vibration of carboxyl group, while the bands at 1486 and 1404 cm^{-1} correspond to the (C=C) stretching in the backbone of the aromatic phenyl ring [45, 48]. Moreover, other folic acid absorption bands at 1606, 1338, and 1188 cm^{-1} observed in folic acid-LDH are assigned to N–N and C–H vibration, respectively [48, 49]. Therefore, it is clear that folic acids have successfully intercalated into LDH.

Figure 5 shows the UV–vis absorption spectroscopy of all samples. The folic acid shows the characteristic absorption peak at approximately 280 nm and broad peak at 350 nm, similar to the literature reported [50]. The typical absorption band of the folic acid-LDH nanohybrid exhibits a small red shift attributed to the transitions of $\pi \rightarrow \pi^*$ in carboxylate [51], which suggests folic acids are intercalated and stabilized by electrostatic interaction with positively charged layers of LDH. In comparison with them, neither the ternary metal Mg/Zn/Al-LDH nor binary metal Mg/Al-LDH shows the absorption peak at 285 nm.

Thermal stability

The TG and DTA curves of pristine LDH, folic acid and folic acid-LDH nanohybrid are depicted in Fig. 6. For pure folic acid, two main weight losses are observed (Fig. 6a). The first step occurred in the temperature around 100 °C arising from the dehydration, accompanied with an endothermic DTA peak at 103 °C. The other extensive weight loss stage, in the temperature range of 200–650 °C, mostly attributed to the decomposition of folic acid [52]. There are two broad endothermic peaks (255 and 588 °C) and an exothermic peak at 310 °C in the DTA curve correspondingly. By comparison, the TG curve of folic acid-LDH shows three noticeable thermal events (Fig. 6b). The first main weight loss with two small endothermic peaks (108 and 200 °C) occurs from 50 to 300 °C. It is mainly owing to the evaporation of adsorbed and interlayer water,

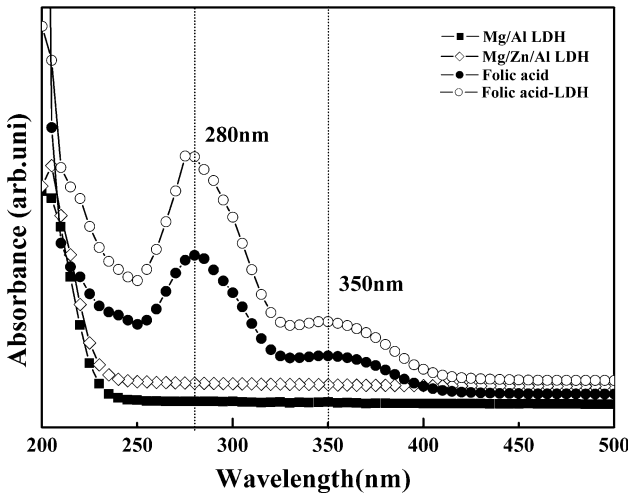

Fig. 5 UV–vis spectra for the folic acid, folic acid-LDH, and LDH

overlapping with trace dehydroxylation of LDH layer [46]. The following mass loss (300–500 °C) is attributed to dehydroxylation of the hydroxide layer and thermal degradation of intercalated folic acid molecules [53]. Correspondingly, the DTA curve shows two small endothermic peaks (397 and 490 °C) and a broad radiative one at 442 °C. The last step (500–600 °C) which accompanied with an exothermic peak at 600 °C is mostly resulted from the strong combustion of intercalated folic molecule. All these temperatures are higher than the decomposition temperature of pure folic acid, which demonstrates the thermal stability of intercalated folic acid molecule was enhanced. It is confirmed that LDH hosts have stable electrostatic interaction with folic acid. Furthermore, the major weight loss of folic acid-LDH in the temperature ranging from 250 to 600 °C is approximately 47.2%, which is similar to the loading amount of folic acid measured by UV–vis spectroscopy (45.2%, Table 1). As shown in the Fig. 6c, the weight loss of Mg/Zn/Al-LDH is similar to the folic acid-LDH, attributed to the removal of surface-absorbed and interlamellar water and the dehydroxylation of host layers, respectively.

Buffer effect of folic acid-LDH

Gastric fluids were mimicked to study the buffer effect of folic acid-LDH nanohybrids by monitoring the changes on the pH values with the addition of 1 M HCl [39]. Figure 7 depicts the correlation between pH value and volume of added HCl. The pH curves of all samples show a profound buffering property when pH value is around 4. The neutralizing and buffering capabilities of folic acid-LDH nanohybrid might come from its hydroxyl groups in the layer, and this function verifies LDH's effective role of antacid, which is also described in previous study [19].

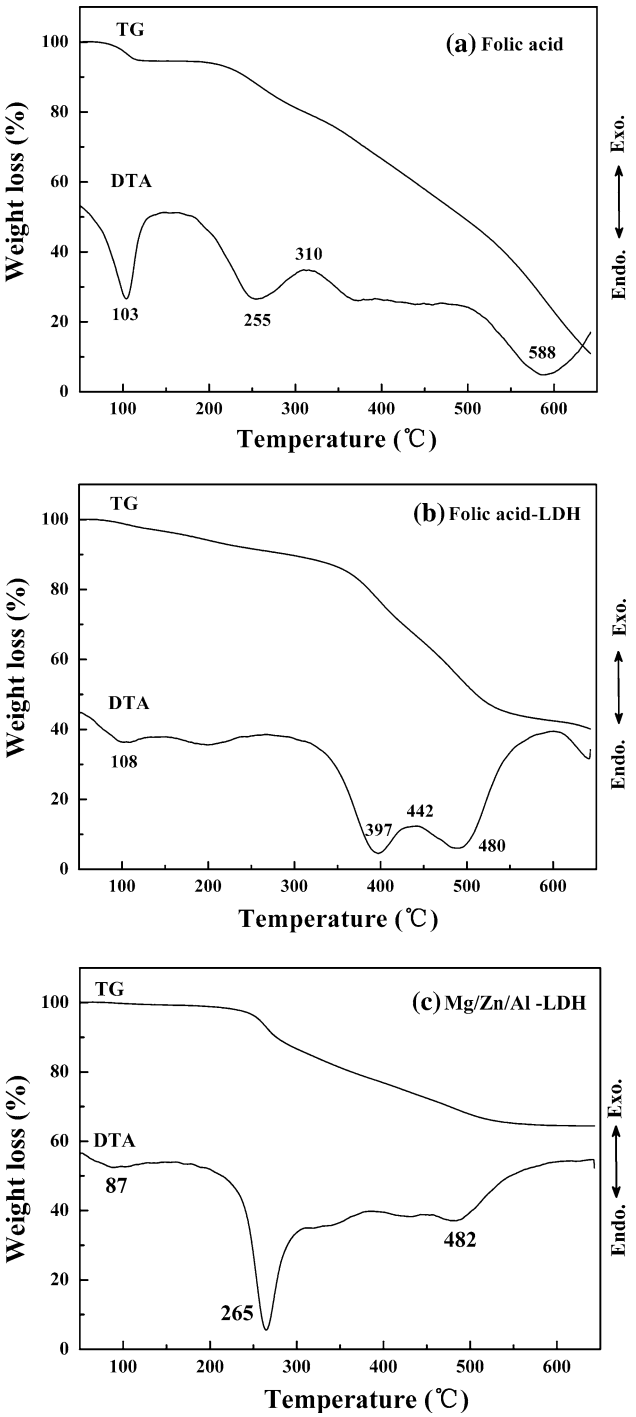

Fig. 6 TG–DTA curves for **a** folic acid, **b** folic acid-LDH, and **c** LDH

Thus, LDH is an ideal antacid to prompt the available folic acid diffusion in simulated gastric fluid.

In vitro release of folic acid-LDH

The release profiles for folic acid-LDH nanohybrid and physically mixed powder are presented in Fig. 8. LDH can

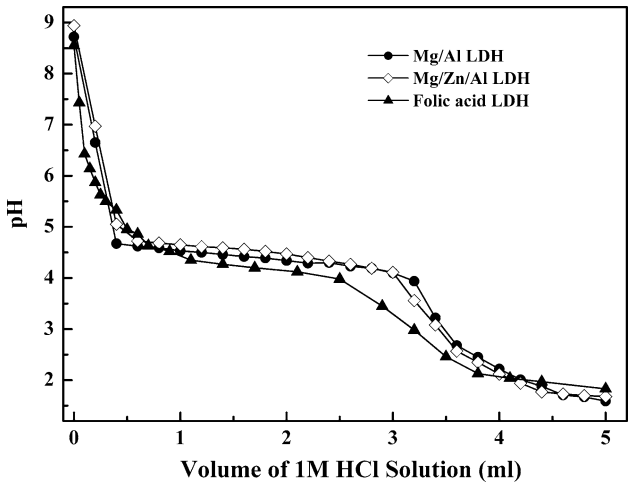

Fig. 7 Titration curves of folic acid-LDH and LDH (*V* represents the added volume of 1 M HCl aqueous solution)

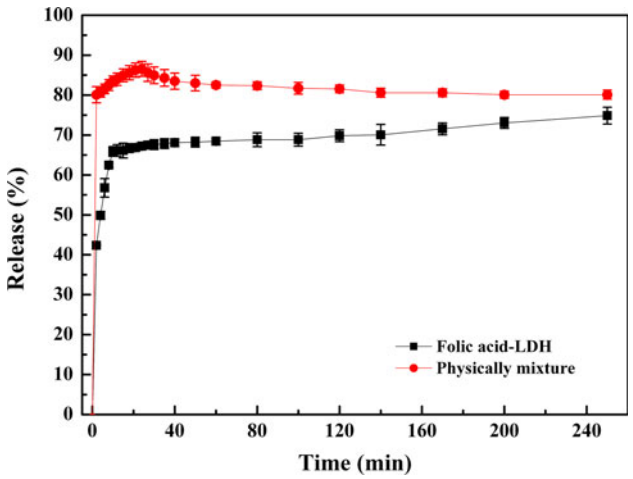

Fig. 8 Release profiles of folic acid from folic acid-LDH and physically mixed powder of folic acid and Mg/Zn/Al-LDH (2/3 weight ratio)

significantly extend the release time of folic acid in buffer. As to the physical mixture of folic acid and LDHs, the released rate reached 87% immediately after 25 min, due to weak electrostatic interaction between folic acid molecules and LDH surface. Thereafter a slow decline of folic acid was observed with only 80% folic acid left in solution after 250 min, which may be attributed to the intercalation of folic acid into LDH similar to the release of other drugs from physical mixture reported in literature [26]. As to the folic acid-LDH, the release curve showed a burst release of only 67% during first 25 min when compared to the 87% of physical mixture. And that initial burst is probably arose from the release of the folic acid that adsorbed in the surface of LDH particles. A more persistent and gradual release process occurred subsequently with released percentage of 67, 70, and 75% after 25, 100, and 250 min, respectively. The following sustained release may be explained by the ion-exchange reaction between the intercalated folic acid anions and phosphate anions in the buffer [22, 24, 47]. In a word, it can be concluded that folic acid-LDH shows an obvious effect of sustained release of folic acid. This nanomaterial could help increase the practical delivery activity of folic acid as the literature reported [54].

As reported, the mechanism of release based on drug-LDHs system could be either diffusion- controlled or dissolution-controlled by LDH particles [47]. In order to explore the release mechanism, we applied four kinetics models to fit the release kinetic data (Fig. 9), and calculated the corresponding linear correlation coefficients (R^2) (Table 2). Compared with the other kinetics models, the parabolic diffusion model is the most fitted model for the release of folic acid, which is reflected by the obviously higher linear correlation coefficient of $R^2 = 0.98$. As the parabolic diffusion model describes intraparticle diffusion or surface diffusion [40], the simulation results in this study suggest that the release process based on folic acid-LDH is controlled by the diffusion of folic acid anions from inside to the surface of LDH particles.

Cytotoxicity of LDH nanohybrids

Figures 10 and 11 show the viability of HEK293T cells in the presence of different nanohybrids at various concentration and incubation times, respectively. The rate of living cell is kept around 90% after incubated with free folic acid and pristine LDH for 48 h at different concentrations. In comparison with them, folic acid-LDH almost has no significant suppression efficiency. No obvious cytopathologic effect is observed (Fig. 10).

Figure 11 exhibits the viability of cells treated with folic acid-LDH decreased slightly when incubated after 72 h at a concentration of 100 μg/mL. Similar results were found when cells were treated at other concentrations for respective time. Although the cells viability shows a low degree of decrease by the incubation time-dependent, the survival rate maintains over 80% which represents the irreversible damage threshold of cell membrane [55]. Figure 12 shows the cell viability of HEK293T after nanohybrid treatment for 72 h using the measurement of lactate dehydrogenase activities. It indicated that the loss of membrane integrity is below 20%, which is consistent with the result of MTT assay.

Therefore, it can be confirmed that the folic acid-LDH is hardly harm to 293T cells after 72 h incubation, and can serve as a noncytotoxic drug delivery system. The overall results demonstrate LDH is an appropriate and promising delivery vector for folic acid.

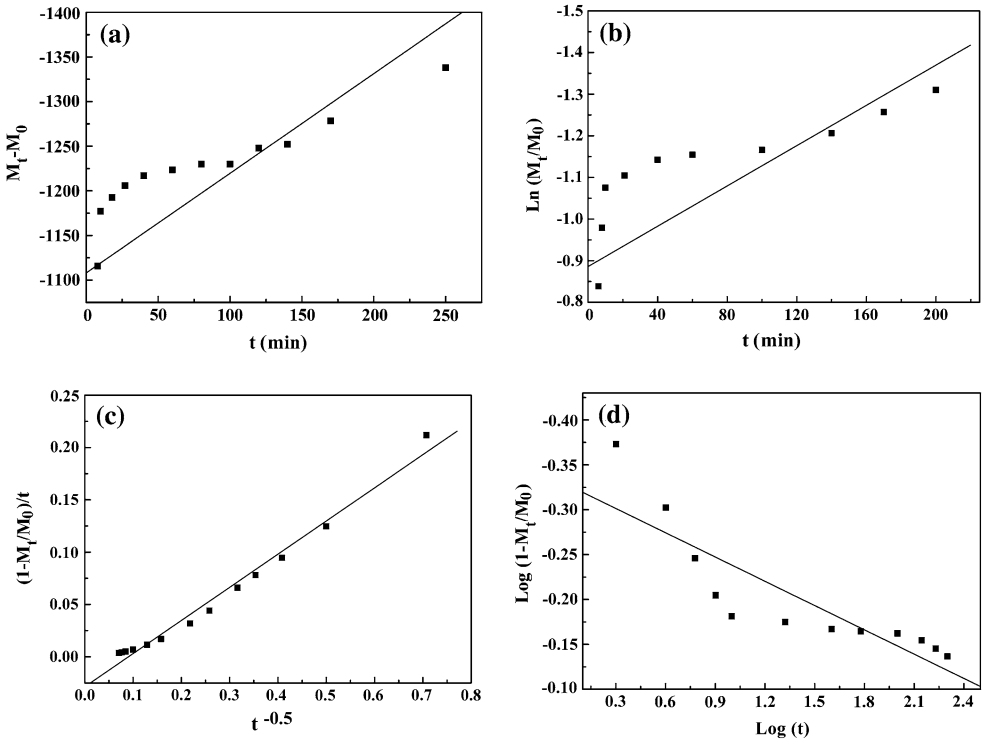

Fig. 9 Fitting the folic acid release data to different kinetic equations **a** Zero-order, **b** First-order, **c** Parabolic diffusion model, and **d** Modified Freundlich model

Table 2 Rate constants and correlation coefficients of the Dissolution–Diffusion Kinetic Models applied to folic acid release from folic acid-LDH based on several models

Kinetic model	Kinetic equation	R^2	k	a
Zero-order	$M_t - M_0 = kt + a$	0.46300	0.08944	58.00651
First-order	$\mathrm{Ln}(M_t/M_0) = -kt + a$	0.54873	0.00242	−0.88601
Parabolic diffusion model	$(1 - M_t/M_0)/t) = kt^{-0.5} + a$	0.98244	0.31690	−0.02864
Modified Freundlich model	$1 - M_t/M_0 = kt^a$	0.75546	0.51630	0.06968

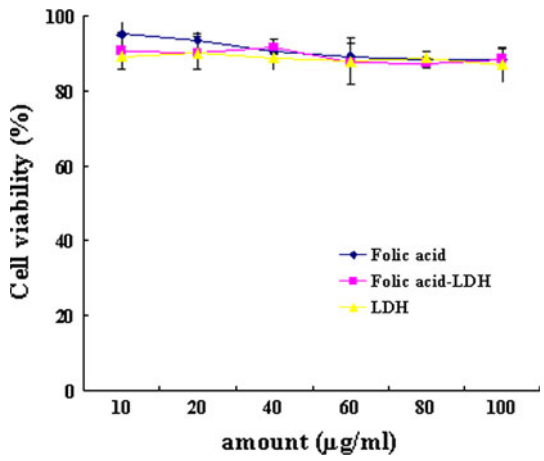

Fig. 10 The effect of folic acid, folic acid-LDH, and LDH on the growth of HEK293T cell. The cells were treated with one of three agents for 48 h

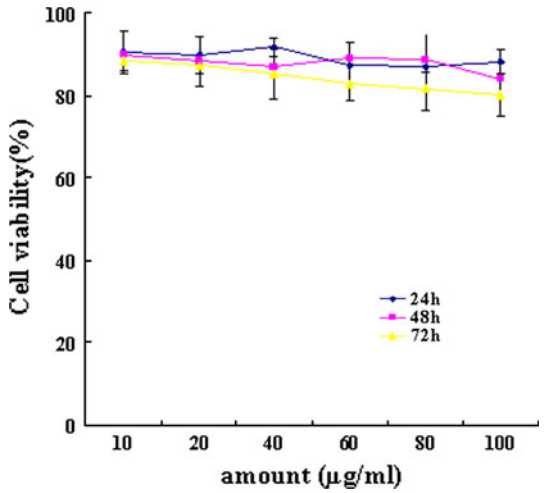

Fig. 11 The effect of folic acid-LDH on the growth of 293T cell. The cells have been treated for 24, 48, and 72 h, respectively

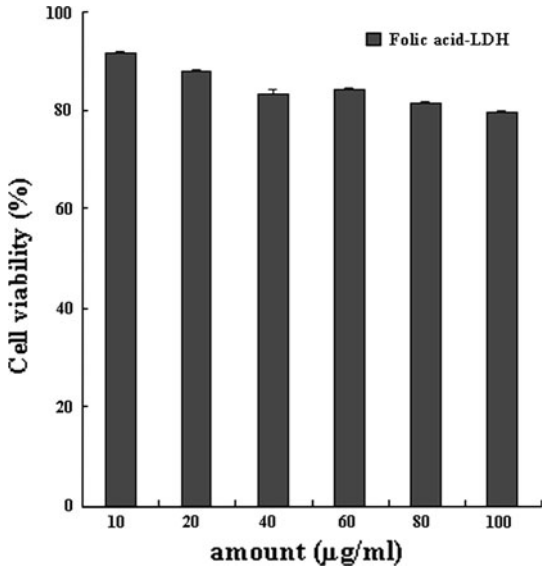

Fig. 12 The cell viability of HEk293T cell measured by lactate dehydrogenase activity. The cells have been treated with folic acid-LDH for 72 h

Conclusion

In this study, folic acid has been successfully intercalated into Mg/Zn/Al-LDH with expanded (003) spacing in XRD patterns. FT-IR spectra also show characteristic bands of folic acid in folic acid-LDH, while TG–DTA curve demonstrates an increased thermal stability of folic acid. The entrapment ratio is 45.1% w/w, and the folic acid anions were released in a sustained way mainly involved in the surface and bulk diffusion. In addition, the good buffer effect in low pH media and non-toxic to normal HEK293T cell proved that folic acid-LDH is a biocompatible antacid matrix. On the basis of these results, Mg/Zn/Al-LDH can be considered as a good nanocarrier to protect and improve the diffusion of folic acid.

Acknowledgements This study was financially supported by the 973 project of the Ministry of Science and Technology (No. 2010CB912604, 2010CB933901), the National Natural Science Foundation of China ((No. 30971631, 30971323), and Doctoral Fund of Ministry of Education of China (No. 20090072120019).

References

1. Scott JM, Kirke PN, Weir DG (1992) Ir J Med Sci 161(10):579
2. Green NS (2002) J Nutr 132(8 Suppl):2356S
3. Molloy AM (2005) Trends Food Sci Technol 16(6–7):241. doi:10.1016/j.tifs.2005.03.009
4. Eichholzer M, Tonz O, Zimmermann R (2006) Lancet 367(9519):1352. doi:10.1016/S0140-6736(06)68582-6
5. Lobo A, Naso A, Arheart K, Kruger WD, Abou-Ghazala T, Alsous F, Nahlawi M, Gupta A, Moustapha A, van Lente F, Jacobsen DW, Robinson K (1999) Am J Cardiol 83(6):821. doi:10.1016/S0002-9149(98)01041-8
6. Alvares Delfino VD, de Andrade Vianna AC, Mocelin AJ, Barbosa DS, Mise RA, Matsuo T (2007) Nutrition 23(3):242. doi:10.1016/j.nut.2007.01.002
7. Carnicer R, Navarro MA, Arbones-Mainar JM, Acin S, Guzman MA, Surra JC, Arnal C, de Las Heras M, Blanco-Vaca F, Osada J (2007) Life Sci 80(7):638. doi:10.1016/j.lfs.2006.10.014
8. McRae MP (2009) J Chiropr Med 8(1):15. doi:10.1016/j.jcm.2008.09.001
9. Mao G, Hong X, Xing H, Liu P, Liu H, Yu Y, Zhang S, Jiang S, Wang X, Xu X (2008) Nutrition 24(11–12):1088. doi:10.1016/j.nut.2008.05.009
10. Shrubsole MJ, Jin F, Dai Q, Shu XO, Potter JD, Hebert JR, Gao YT, Zheng W (2001) Cancer Res 61(19):7136
11. Jennings E (1995) Med Hypotheses 45(3):297
12. Du W, Li WY, Lu R, Fang JY (2010) World J Gastroenterol 16(8):921
13. Fenech M (2001) Mutat Res 475(1–2):57
14. Lazarou C, Kapsou M (2010) Complement Ther Clin Pract 16(3):161. doi:10.1016/j.ctcp.2010.01.003
15. Abou-Saleh MT, Coppen A (2006) J Psychosom Res 61(3):285. doi:10.1016/j.jpsychores.2006.07.007
16. Younis IR, Stamatakis MK, Callery PS, Meyer-Stout PJ (2009) Int J Pharm 367(1–2):97. doi:10.1016/j.ijpharm.2008.09.028
17. Sculthorpe NF, Davies B, Ashton T, Allison S, McGuire DN, Malhi JS (2001) J Public Health Med 23(3):195
18. Lue Z, Zhang FZ, Lei XD, Yang L, Xu SL, Duan X (2008) Chem Eng Sci 63(16):4055. doi:10.1016/j.ces.2008.05.007
19. Del Hoyo C (2007) Appl Clay Sci 36(1–3):103. doi:10.1016/j.clay.2006.06.010
20. Chen T, Xu SL, Zhang FZ, Evans DG, Duan X (2009) Chem Eng Sci 64(21):4350. doi:10.1016/j.ces.2009.07.005
21. Ladewig K, Xu ZP, Lu GQ (2009) Expert Opin Drug Deliv 6(9):907. doi:10.1517/17425240903130585
22. Pan DK, Zhang H, Zhang T, Duan X (2010) Chem Eng Sci 65(12):3762. doi:10.1016/j.ces.2010.03.013
23. Gasser MS (2009) Colloids Surf B Biointerfaces 73(1):103. doi:10.1016/j.colsurfb.2009.05.005
24. Ambrogi V, Perioli L, Ciarnelli V, Nocchetti M, Rossi C (2009) Eur J Pharm Biopharm 73(2):285. doi:10.1016/j.ejpb.2009.06.007
25. Li BX, He J, Evans DG, Duan X (2004) Appl Clay Sci 27(3–4):199. doi:10.1016/j.clay.2004.07.02
26. Gu Z, Thomas AC, Xu ZP, Campbell JH, Lu GQ (2008) Chem Mater 20(11):3715
27. Xue YH, Zhang R, Sun XY, Wang SL (2008) J Mate Sci Mater Med 19(3):1197. doi:10.1007/s10856-007-3221-4
28. Auerbach SM, Carrado KA, Dutta PK (2004) Handbook of layered materials. M. Dekker, New York
29. Rives V (2001) Layered double hydroxides: present and future. Nova Science Publishers, New York
30. Silvério F, dos Reis M, Tronto J, Valim J (2008) J Mater Sci 43(2):434. doi:10.1007/s10853-007-2202-9
31. Naime Filho J, Silvério F, dos Reis M, Valim J (2008) J Mater Sci 43(21):6986. doi:10.1007/s10853-008-2952-z
32. Ho E (2004) J Nutr Biochem 15(10):572. doi:10.1016/j.jnutbio.2004.07.005
33. Maret W, Sandstead HH (2006) J Trace Elem Med Biol 20(1):3. doi:10.1016/j.jtemb.2006.01.006
34. Scheplyagina LA (2005) J Trace Elem Med Biol 19(1):29. doi:10.1016/j.jtemb.2005.07.008
35. Saris NEL, Mervaala E, Karppanen H, Khawaja JA, Lewenstam A (2000) Clin Chim Acta 294(1–2):1
36. Musso CG (2009) Int Urol Nephrol 41(2):357. doi:10.1007/s11255-009-9548-7

37. Xu ZP, Walker TL, Liu KL, Cooper HM, Lu GQM, Bartlett PF (2007) Int J Nanomed 2(2):163
38. Gordijo CR, Barbosa CAS, Ferreira AMDC, Constantino VRL, Silva DD (2005) J Pharm Sci 94(5):1135
39. Tronto J, Crepaldi EL, Pavan PC, De Paula CC, Valim JB (2001) Mol Cryst Liq Cryst 356:227
40. Yang JH, Han YS, Park M, Park T, Hwang SJ, Choy JH (2007) Chem Mater 19(10):2679. doi:10.1021/Cm070259h
41. Mosmann T (1983) J Immunol Methods 65(1–2):55. doi:10.1016/0022-1759(83)90303-4
42. Caviedes-Bucheli J, Avendano N, Gutierrez R, Hernandez S, Moreno GC, Romero MC, Munoz HR (2006) J Endod 32(3):183
43. Valente JS, Hernandez-Cortez J, Cantu MS, Ferrat G, Lopez-Salinas E (2010) Catal Today 150(3–4):340. doi:10.1016/j.cattod.2009.08.020
44. Valente JS, Tzompantzi F, Prince J, Cortez JGH, Gomez R (2009) Appl Catal B Environ 90(3–4):330. doi:10.1016/j.apcatb.2009.03.019
45. Choy JH, Jung JS, Oh JM, Park M, Jeong J, Kang YK, Han OJ (2004) Biomaterials 25(15):3059. doi:10.1016/j.biomaterials.2003.09.083
46. Qin LL, Wang SL, Zhang R, Zhu RR, Sun XY, Yao SD (2008) J Phys Chem Solids 69(11):2779. doi:10.1016/j.jpcs.2008.06.144
47. Hussein MZ, Nasir NM, Yahaya AH (2008) J Nanosci Nanotechnol 8(11):5921
48. Pavia DL, Lampman GM, Kriz GS (2001) Introduction to spectroscopy : a guide for students of organic chemistry, 3rd edn. Fort Worth, Harcourt College Publishers, London
49. Zhang J, Rana S, Srivastava RS, Misra RD (2008) Acta Biomater 4(1):40. doi:10.1016/j.actbio.2007.06.006
50. Off MK, Steindal AE, Porojnicu AC, Juzeniene A, Vorobey A, Johnsson A, Moan J (2005) J Photochem Photobiol B 80(1):47. doi:10.1016/j.jphotobiol.2005.03.001
51. Oh J-M, Choi S-J, Lee G-E, Han S-H, Choy J-H (2009) Adv Funct Mater 19(10):1617
52. Vora A, Riga A, Dollimore D, Alexander KS (2002) Thermochim Acta 392–393:209
53. Li L, Zhang L, Wen Z, Chen D (2010) Chin J Chem 28(2):171
54. Li Y, Liu D, Ai HH, Chang Q, Liu DD, Xia Y, Liu SW, Peng NF, Xi ZG, Yang X (2010) Nanotechnology 13:105101. doi:10.1088/0957-4484/21/10/105101
55. Wei W, Zheng-zhong B, Yong-jie W, Qing-wu Z, Ya-lin M (2004) J Ultrasound Med 23(12):1569